Neurobiology of Disease 76 (2015) 87–97

Contents lists available at ScienceDirect

Neurobiology of Disease

journal homepage: www.elsevier.com/locate/ynbdi

A novel anticonvulsant mechanism via inhibition of complement receptor C5ar1 in murine epilepsy models

Melissa J. Benson [a], Nicola K. Thomas [a], Sahil Talwar [b], Mark P. Hodson [c], Joseph W. Lynch [b], Trent M. Woodruff [a], Karin Borges [a,*]

[a] Department of Pharmacology, School of Biomedical Sciences, The University of Queensland, Skerman Building, St Lucia, Queensland 4072, Australia
[b] Queensland Brain Institute, The University of Queensland, St Lucia, Queensland 4072, Australia
[c] Australian Institute for Bioengineering and Nanotechnology, The University of Queensland, St Lucia, Queensland 4072, Australia

ARTICLE INFO

Article history:
Received 23 October 2014
Revised 21 January 2015
Accepted 4 February 2015
Available online 11 February 2015

Keywords:
Anticonvulsant
Epilepsy
Seizure
Complement
C5a
C5ar1
PMX53
Status epilepticus
Neurodegeneration

ABSTRACT

The role of complement system-mediated inflammation is of key interest in seizure and epilepsy pathophysiology, but its therapeutic potential has not yet been explored. We observed that the pro-inflammatory C5a receptor, C5ar1, is upregulated in two mouse models after status epilepticus; the pilocarpine model and the intrahippocampal kainate model. The C5ar1 antagonist, PMX53, was used to assess potential anticonvulsant actions of blocking this receptor pathway. PMX53 was found to be anticonvulsant in several acute models (6 Hz and corneal kindling) and one chronic seizure model (intrahippocampal kainate model). The effects in the 6 Hz model were not found in *C5ar1*-deficient mice, or with an inactive PMX53 analogue suggesting that the anticonvulsant effect of PMX53 is C5ar1-specific. In the pilocarpine model, inhibition or absence of C5ar1 during status epilepticus lessened seizure power and protected hippocampal neurons from degeneration as well as halved SE-associated mortality. *C5ar1*-deficiency during pilocarpine-induced status epilepticus also was accompanied by attenuation of TNFα upregulation by microglia, suggesting that C5ar1 activation results in TNFα release contributing to disease. Patch clamp studies showed that C5a-induced microglial K^+ outward currents were also inhibited with PMX53 providing a potential mechanism to explain acute anticonvulsant effects. In conclusion, our data indicate that C5ar1 activation plays a role in seizure initiation and severity, as well as neuronal degeneration following status epilepticus. The widespread anticonvulsant activity of PMX53 suggests that C5ar1 represents a novel target for improved anti-epileptic drug development which may be beneficial for pharmaco-resistant patients.

Introduction

Epilepsy is a debilitating disease, especially if seizures cannot be managed with medication. The global prevalence of treatment-resistance within epileptic populations is approximately 35%, highlighting the need for new anti-epileptic treatments effective for these patients (Kwan et al., 2011).

A new approach different from existing anti-epileptic drug (AED) mechanistic pathways is proposed, stemming from recent findings relating inflammation with epilepsy (Vezzani et al., 2011). Anti-inflammatory approaches to block seizures have already shown to be effective, not only in rodent seizure models (Vezzani and Granata, 2005; Maroso et al., 2011) but also in selected drug-resistant patients (Marchi et al., 2011) advocating inflammation as a key pharmacological target to reduce seizures and modify the disease.

The complement cascade is a major component of the innate immune system, and produces a potent inflammatory response when activated (Amara et al., 2010). Recent evidence has linked complement factor expression and activation with epilepsy and seizure development. For example, gene expression studies demonstrated upregulation of various complement factors in surgically removed tissue from patients with temporal lobe epilepsy (TLE), and in rodent TLE models (Becker et al., 2003; Gorter et al., 2006; Jamali et al., 2006; Aronica et al., 2007). Increased immunoreactivity of multiple complement factors, such as C1q, C3, C4, and the membrane attack complex (MAC), consisting of the C5b-9 complex, are documented on activated microglia and select neurons in brain tissue from TLE patients and rodent TLE models (Aronica et al., 2007; Kharatishvili et al., 2014). The presence of MAC strongly suggests complement cascade activation in "epileptic tissue", which includes C5a formation. Moreover, in untreated people

* Corresponding author at: Skerman Building, School of Biomedical Sciences, The University of Queensland, St Lucia Campus, Brisbane, Queensland 4072, Australia.
E-mail address: k.borges@uq.edu.au (K. Borges).
Available online on ScienceDirect (www.sciencedirect.com).

http://dx.doi.org/10.1016/j.nbd.2015.02.004
0969-9961/

with epilepsy, significantly increased C3 serum levels were found compared to healthy and epileptic control patients, indicating complement involvement in seizures (Başaran et al., 1994).

There is also functional evidence that complement in the brain may contribute to seizure generation. The presence of specific genetic polymorphisms in the C3 promoter region was significantly greater in mesial TLE patients and correlated with increased febrile seizure susceptibility (Jamali et al., 2010). In addition, sequential infusion of individual C5b-C9 complement proteins into the rat hippocampus resulted in MAC immunoreactivity and induced seizures and neurodegeneration (Xiong et al., 2003). Recently, it was also reported that C5a receptor (C5ar1) expression on microglia was upregulated following excitotoxic kainate insult and is controlled by FosB, a mediator of transcriptional activator AP-1 (Nomaru et al., 2014). Deletion of *FosB*, and hence lack of C5ar1 upregulation also reduced pro-inflammatory cytokine expression following the insult. These studies provide evidence that complement presence and/or activation in the brain can mediate changes relevant to seizure generation and epilepsy pathophysiology.

In this study, we aimed to identify the therapeutic potential of inhibiting complement-mediated inflammation using several epilepsy models. We focussed on the complement peptide C5a, an inflammatory mediator. It is produced from proteolytic cleavage of its precursor C5, typically via C5 convertases formed from C3 during complement cascade activation. C5a is extremely potent at stimulating immune cell recruitment and subsequent activation through its receptor C5ar1, and induces production of pro-inflammatory cytokines and mediators (Woodruff et al., 2010).

Here, we used the selective cyclic hexapeptide C5ar1 antagonist, PMX53 (Wong et al., 1998; Finch et al., 1999) to assess the role of C5ar1 activation in seizures and epilepsy pathophysiology. Binding studies have demonstrated that PMX53 binds to and inhibits C5ar1 with high affinity (~20 nM). Also, PMX53 did not alter the action of closely related inflammatory mediators including fMet-Leu-Phe, leukotriene B4, platelet-activating factor, C3a, or IL-8 (March et al., 2004). Furthermore, it has been shown that PMX53 does not inhibit the binding of C5a to the second, alternative C5a receptor, C5ar2 (Scola et al., 2007). Preclinically PMX53 has been neuroprotective in several neurological disease models, including Huntington's disease, amyotrophic lateral sclerosis, traumatic brain injury, stroke, and spinal cord injury (Sewell et al., 2004; Woodruff et al., 2006, 2008, 2010; Kim et al., 2008; Li et al., 2014).

We identified the effects of *C5ar1* inhibition and absence in several models of experimental epilepsy revealing that it may provide new avenues for AED discovery, specifically for pharmaco-resistant patients.

Materials & methods

Mice

8–10 week old male Swiss CD1 mice (Animal Resources Centre, Western Australia) were singly housed with a 12 h light/dark cycle and access to food and water *ad libitum*. Male C57BL/6 *C5ar1*-deficient mice were bred into the CD1 background at The University of Queensland (UQ). CD1 mice were obtained from Animal Resource Centre (Perth, Australia). Initial *C5ar1*-deficient breeding pairs were obtained from Trent Woodruff (UQ) and were originally described by Hollmann et al. (2008). After five generational crosses, male mice were used. *C5ar1*-deficiency was verified by standard PCR genotyping methods. All experiments were approved by the UQ Animal Ethics Committee and conducted in accordance with their guidelines. All experiments were performed with experimenters blinded to treatment/genotype.

Drugs

PMX53 (AcF-[OP(D-Cha)WR]) and PMX203 (AcF-[OPGWR]) were synthesized as described (Finch et al., 1999; Woodruff et al., 2005). PMX53 was provided by Cephalon (Australia). After dissolving in 3.75% ethanol (at 0.75 mg/ml), PMX53 was administered subcutaneously 30 min prior to seizure induction unless otherwise stated.

Liquid chromatography tandem mass spectrometry (LC–MS/MS)

Plasma and perfused whole brain samples were extracted as described (Strachan et al., 2001). HPLC Grade acetonitrile and formic acid (AR Grade) was purchased from RCI Labscan (Bangkok, Thailand) and Labscan (Gliwice, Poland) respectively. Deionised water was generated via an Elga Purelab Classic water purification unit (Veolia Water Solutions and Technologies, Saint-Maurice Cedex, France).

Liquid chromatography tandem mass spectrometry (LC–MS/MS) data were acquired on a Dionex UltiMate 3000 liquid chromatography system (Dionex, Sunnyvale, CA) coupled to an ABSciex 4000 QTRAP mass spectrometer (ABSciex, Concord, Canada). The liquid chromatography system was controlled by Chromeleon software (v6.80, Dionex), and chromatographic separation was achieved by injecting 10 µl onto a Gemini-NX C18 150 mm × 2 mm I.D., 3 µm 110 Å particle column (Phenomenex, Aschaffenburg, Germany) equipped with a pre-column Security Guard Gemini-NX C18 4 mm × 2 mm I.D. cartridge. The column oven temperature was controlled and maintained at 60 °C throughout the acquisition. The mobile phase flow rate was maintained at 300 µl/min for 5 min and the mobile phase (isocratic) was 50:50 (*v*/*v*) purified water:acetonitrile plus 0.1% (*v*/*v*) formic acid.

The mass spectrometer was controlled by Analyst software (v1.5.2, ABSciex) and was equipped with a TurboV electrospray source operated in positive ion mode. The following optimized parameters were used to acquire Multiple Reaction Monitoring (MRM) data: ionspray voltage 5300 V, nebulizer (GS1), auxiliary (GS2), curtain (CUR) and collision (CAD) gases were 40, 80, 15 and high (arbitrary units), respectively, generated via a N300DR nitrogen generator (Peak Scientific, Massachusetts, USA). The auxiliary gas temperature was maintained at 420 °C. The analyte-dependent parameters for the detection of PMX53 are given in Table 1. For all analytes the entrance potential (EP) was 10 V.

The samples were run with sample- and analyte-relevant calibration standards and pooled QC samples (Sangster et al., 2006; Hodson et al., 2009) to control for reproducibility of data acquisition and to ensure data integrity. Analyte stock solutions were prepared in purified water (Veolia). Data were processed and analysed in Analyst 1.5.2 and MultiQuant 2.1 (ABSciex).

Animal seizure models

6 Hz test

0.5% tetracaine (Sigma Aldrich, Australia) in 0.9% saline was applied to both corneas of the mice. Corneal electroshocks from a rodent electroshock unit (Ugo Basile, Varese, Italy; 6 Hz, 3 s, 0.2 millisecond rectangular pulse width) were given starting at 14 mA (Samala et al., 2008). Using the up down method we determined the critical current at which 50% of mice seized (Thomas et al., 2012).

Corneal kindling model

Electroshocks (50 Hz, 0.4 millisecond pulse) to the tetracaine-anaesthetised corneas were administered twice per day for 20 days using a rodent electroshock unit (Ugo Basile). A single seizure was experienced by each mouse as a result of a single kindling stimulus. Seizures were scored as previously described (Willis et al., 2010).

Pilocarpine status epilepticus (SE) model

Based on the protocol described by Borges et al. (2003), mice were injected with methyl-scopolamine (2.5 mg/kg *i.p.* in 0.9% NaCl) 15 min prior to 345 mg/kg (*s.c.*) pilocarpine, which induced SE in >60% of mice. Ninety minutes post-pilocarpine all mice received 30 mg/kg (*i.p.*) pentobarbitone to stop seizures. Post-SE, mice received 1 ml 4% dextrose twice daily (*s.c.*) and health was monitored (Smeland et al., 2013). 3 days later animals were perfused and brains fixed with 4%

Table 1
Analyte-dependent parameters for the transitions used in Multiple Reaction Monitoring data acquisition.

Analyte	Q1 mass (daltons)	Q3 mass (daltons)	Dwell time (milliseconds)	DP (volts)	CE (volts)	CXP (volts)
PMX53 (quantifier)	896.2	69.9	50	151	129	2
PMX53 (qualifier 1)	896.2	158.9	50	151	89	8
PMX53 (qualifier 2)	896.2	223.4	50	151	87	12

Key: Q — quadrupole; DP — declustering potential; CE — collision energy; and CXP — collision cell exit potential.

paraformaldehyde. For EEG experiments, electrodes were implanted >1 week before recording (see *i.h.* kainate model).

Intrahippocampal (i.h.) kainate model

Based on the protocol described by Gouder et al. (2003), briefly, mice were deeply anesthetised with 1.8% isoflurane mixed with oxygen (Troylab, Glendenning, Australia). Eighty nanolitres of 20 mM kainic acid (~1.7 nmol, Sigma Aldrich) was stereotaxically (Kopf, Tujunga, California) injected unilaterally into the hippocampal CA1 pyramidal cell layer (AP −1.94, ML −1.25, DV −1.5 from bregma) using a 0.1 μl microsyringe (Hamilton, Reno, NV) attached to a 0.28 mm stainless steel cannula via PE20 tubing (Plastics One, Roanoke, VA). After awakening, mice underwent SE for a continuous period >3 h. Three weeks later, a unilateral bipolar depth electrode (formed from two twisted enamel-coated insulated stainless steel 170 μm diameter wires, 0.4 mm tip separation, Plastics One) was implanted stereotaxically into the same site, along with 3 stainless steel surface screw electrodes (1.2 mm diameter, Plastics One). Two were placed bilaterally 2.5 mm posterior to the lambda and one was placed over the contralateral (3 mm from midline) frontal cortex 1 mm posterior to bregma, to act as ground and reference (including cortical reference) electrodes. Electrode wires were mounted into a multichannel electrode pedestal (MS363, Plastics One) and secured with dental cement. Mice recovered for >1 week prior to EEG recordings.

Video electroencephalographic (EEG) recording of seizures

EEG was recorded with a sampling frequency of 512 Hz (E-Series EEG system with Profusion 4 software, Compumedics, Melbourne, Australia) and analysed using Labchart 8 custom seizure detection and analysis software involving Matlab calculations (AD Instruments, Bella Vista, Australia). Seizure detection involved six digital filtering steps from raw EEG output and detected seizure events within the 6–12 Hz bandwidth. All seizures were confirmed using parallel video recording by a blinded experimenter. Seizure frequency is reported as the number of seizure events per minute. Seizure power is defined as the signal intensity of the EEG trace given in unit μV^2 over a defined time period (a seizure or SE). Seizure power was quantified using Labchart to calculate the sum of the area under the curve based on EEG trace amplitude for defined time periods (seizures/SE). This value gave power for an individual seizure, which was then calculated for all seizures for each mouse and averaged. Seizure power is reported as an average for each individual animal normalized to baseline to compare treatment groups. SE seizure power is reported as an average for each treatment group.

Typically pilocarpine-SE mice experienced severe clonic seizures often including loss of balance, whilst kainate-SE mice experienced partial forelimb clonus with head bobbing most commonly. However some generalised seizures were also recorded in kainate-SE mice. Exclusion criteria: seizures <10 s in length; mice with baseline changes of >50% total seizure time between recording weeks.

Fluoro-Jade B (FJB) staining

Coronal 9 μm paraffin brain sections were stained as described (Schmued and Hopkins, 2000). Degenerating cells were visualized on an upright fluorescent microscope (Axio Imager, Zeiss, Jena, Germany) and images captured for each slide at 20× magnification. For each animal three 9 μm sections of medial hippocampus were analysed. We averaged FJB-positive cell number for each mouse based on automated spot detection of all sections (including both hemispheres) using Imaris software (BitPlane, Belfast, UK). Spots were automatically detected based upon cell size, shape and fluorescence intensity and were verified for each slide by eye to ensure false-positives were not detected. The total area of each region of the hippocampal formation in the 2D plane was outlined in the programme and calculated in mm^2. From this count we then determined the total number of FJB-positive cells per area (mm^2) for each region of the hippocampal formation (CA1, CA3, DG) for each individual mouse. Average values for a total group of mice ($n = 14$–20 per group) were then reported in Figs. 4i & j. NoSE animals were used at conditional controls for all experiments.

Flow cytometry

Forebrain cells from two PBS-perfused mice were isolated and pooled. Cells were incubated with a cocktail containing Alexa Fluor 488 — anti-C5ar1 (MCA2456A488, AbD Serotec), PE-Cyanine 7 — anti-CD45 (25-0451, eBioscience), BD Horizon V450 — anti-Ly-6G (560603, BD Bioscience) and non-conjugated anti-CD16/32 (16-0161, eBioscience) for 20 min at 4 °C before fixation. For IL-1β and TNFα, cells were pre-incubated for 3 h in RPMI medium containing β-mercaptoethanol and Brefeldin A (1:1000) with 10% Foetal bovine serum then incubated in antibody cocktail. Cells were fixed and permeabilised prior to incubation with APC-conjugated — anti-IL-1β (17-7114, eBioscience) or PE-conjugated — anti-TNFα (554419, BD Pharmingen) for 45 min at RT. Cells were analysed using a BD LSRII flow cytometer (BD Biosciences, San Jose, CA) and BD FACSDiva software.

Real-time quantitative polymerase chain reaction (qPCR)

Forebrains (pilocarpine) or hippocampus (kainate model) were dissected from saline-perfused brains. After RNA extraction (RNAeasy MiniPrep, Qiagen, Hilden, Germany), DNase I treatment (Promega, Madison, Wisconsin) and determination of concentrations, cDNA was synthesised (Tetro kit, Bioline, Alexandria, Australia). qPCRs were performed with gene-specific primers spanning across an intron and SYBR green reagents (Applied Biosystems, Foster City, CA) on a Viia7 machine (Applied Biosystems) with Tata Box protein and hydroxymethylbilane synthase as housekeeping genes and glyceraldehyde-3-phosphate dehydrogenase as control for DNA contamination.

Microglial cell culture

Briefly, forebrains were isolated from E17 CD1 mouse embryos and the meninges removed. Tissue was digested with 0.5% trypsin solution and then incubated with 1% trypsin inhibitor (Sigma Aldrich, St. Louis, MO). Cells were dissociated via trituration and plated at 3×10^5 cells/ml density in poly-D-lysine (PDL) coated culture flasks with 1:1 Dulbecco's modified Eagle's medium (DMEM) with Ham's F12 nutrient containing 10% foetal bovine serum and antibiotics (penicillin, streptomycin, 25 U/ml final). Mixed glial cells were cultured for approximately 2 weeks until the underlying astrocyte layer was confluent, during which time frequent media changes occurred. No neurons were present in this culture. At this time, microglial cells were separated from astrocytes by shaking and allowed to adhere to PDL-coated glass coverslips maintained in macrophage serum-free medium supplemented with 20% astrocyte conditioned medium (DMEM cultured for 3 days with astrocyte-only cultures and filtered). Isolated microglia were maintained for 2 days prior to use in patch clamp experiments. All tissue

culture mediums and reagents were obtained from Life Technologies, Carlsbad, CA.

Patch clamping

The procedure was modified from Ilschner et al. (1996). Coverslips were placed on the stage of an inverted microscope (CKX4ISF, Olympus Ltd., Japan) and superfused with standard extracellular solution (KCl 5.4, NaCl 150, $MgCl_2$ 1, $CaCl_2$ 2, glucose 10, HEPES 10 at pH 7.3 adjusted with KOH). Whole cell recordings were made using the patch-clamp technique in the whole cell voltage clamp configuration using an Axon Multiclamp 700B (Molecular Devices LLC, Sunnyvale, CA). Patch pipettes were pulled from borosilicate glass (GC150F-7.5, Harvard Apparatus, UK) with a vertical micropipette puller (PC10, Narishige, Japan). The resistance of pipettes was 4–5 MΩ. The standard recording pipette solution contained (in mM): KCl 130, $CaCl_2$ 1, $MgCl_2$ 1, EGTA 10 mM, HEPES 10 mM, ATP 2 mM at pH 7.4 adjusted with KOH. The series resistance was compensated by 40–50% prior to recordings and cells were held at −70 mV. When measuring potassium currents, voltage steps with 35 mV increments were applied for 100 ms from a holding potential of 0 mV in both depolarising and hyperpolarising directions. Currents were digitized at 10 kHz and filtered at 2 kHz. Mouse recombinant C5a (20 nM, R&D systems, Minneapolis, MN) and PMX53 (100 nM) were applied via a continuous gravity perfusion system.

Statistical analysis

Statistical tests completed using GraphPad Prism 6.0 software (La Jolla, CA) are detailed for each data set in the results. Post-hoc Bonferroni multiple comparisons test was used for all ANOVA analysis.

Results

C5ar1 antagonist, PMX53, reached the CNS in levels equivalent to the IC_{50}

LC–MS/MS analysis of plasma and brain tissue after PMX53 injection (3 mg/kg, *s.c.*) showed that circulating PMX53 levels were highest at the measurement timepoint 15 min post-injection at 432 ng/ml (~480 nM) and were rapidly depleted by 90 min (Fig. 1a), with no drug detectable in the plasma or brain after 4 h (data not shown). 15 ng/g of PMX53 was found in perfused brain tissue at 30 min post-injection, equating to approximately 20 nM in brain extracellular fluid, the IC_{50} for the drug at the C5a receptor (Finch et al., 1999) (Fig. 1b). This pharmacokinetic profile correlates well with the protective effects described below, as maximal anticonvulsant action in the 6 Hz test was observed 30 min post-administration, when the IC_{50} of PMX53 was present, which was diminished by 20% 60 min post-administration and absent after 90 min (data not shown). For this reason the 30 minute timepoint was chosen as the optimal pre-treatment timeframe for further PMX53 anticonvulsant experiments.

PMX53 significantly reduces electroencephalographic spontaneous seizures in the chronic i.h. kainate epilepsy model

Significant improvements in seizure behaviour were found with single PMX53 administration (*s.c.*) to chronically epileptic mice in the intrahippocampal kainate model compared to vehicle. In a paired cross-over design, each animal was injected with PMX53 and vehicle one week apart, with half of the group receiving PMX53 first. Seizure behaviour during a 90 minute period following injection was evaluated relative to a 90 minute baseline recorded before treatment (Figs. 2a, b). A 58% reduction in the total time spent in seizure, as well as a 22% reduction in average seizure power was found with PMX53 treatment, relative to vehicle injection (Figs. 2c, d). Decreased seizure frequencies were seen with PMX53 treatment in the majority of mice (Fig. 2e), but no significant changes to average seizure length were observed between treatments (Fig. 2f).

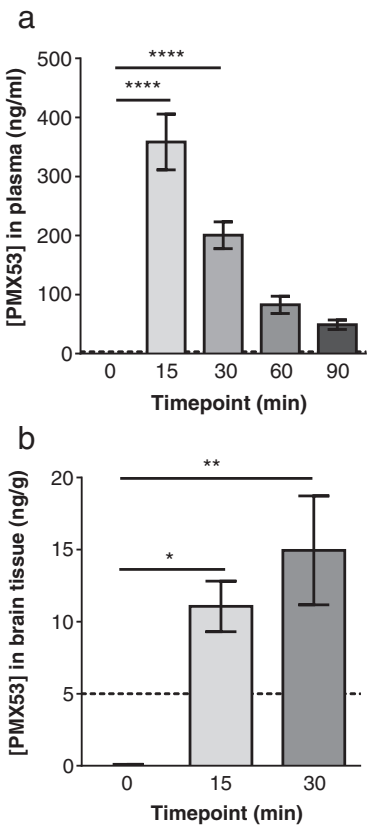

Fig. 1. Levels of PMX53 in plasma and brain following PMX53 injection determined using quantitative LC–MS/MS. (a) Plasma levels of PMX53 peaked 15 min post-injection (****$P < 0.0001$, $n = 6$). The detection limit was 3 ng/ml plasma as indicated by the dotted line. (b) Levels of PMX53 in brain tissue peaked at 30 min (*$P = 0.0015$, $n = 6$). The detection limit was 5 ng/g. All data were corrected for extraction efficiency; plasma 83%, brain tissue 96%. One way ANOVA with Bonferroni post-test was used for both data sets. Data expressed as mean ± SEM.

At both 3 and 21 days post-kainate-induced SE, we observed significant increases in hippocampal mRNA levels of C5ar1 and C3, central components of the complement cascade, suggesting a consistent presence of complement components throughout the epileptogenic period. Relative to vehicle-injected control mice, mRNA levels of *C5ar1* were increased by 4 and 1.7 fold and those of *C3* by 2.4 and 3.6 fold, respectively (Fig. 2g). Additionally, C3 mRNA, but not C5ar1, was also increased by 4 fold at the chronic 12 month timepoint post-SE compared to vehicle-injected control mice, inferring upregulation of complement once seizures were established (Fig. 2h).

PMX53 is anticonvulsant in a model predisposed to seizures and shows C5ar1-dependent anticonvulsant effects in the 6 Hz model of acute seizures

In the predisposed seizure model, mice were stimulated through their anesthetised corneas until 5 consecutive stage 5 seizures were experienced from 5 independent kindling stimuli, at which time they were considered to be "fully kindled" (Fig. 3a). Thirty minutes before the next kindling stimulus mice were injected with PMX53 (3 mg/kg, *s.c.*) or vehicle. 50% less of the PMX53-treated mice experienced stage 5 seizures compared to the vehicle-treated mice, showing an anticonvulsant effect of PMX53 in this model (Fig. 3b).

In the acute 6 Hz seizure model the effect of PMX53 was maximal 30 min after a single injection (3 mg/kg, *s.c.*) and lost after 90 min (data not shown). The current at which 50% of mice seize (CC50) was increased on average by 6.6 mA ± 1.6 relative to vehicle-injected mice (Fig. 3c).

To determine if this anticonvulsant effect in the 6 Hz model (Fig. 3c) was C5ar1-dependent, we injected in parallel, an inert structural analogue

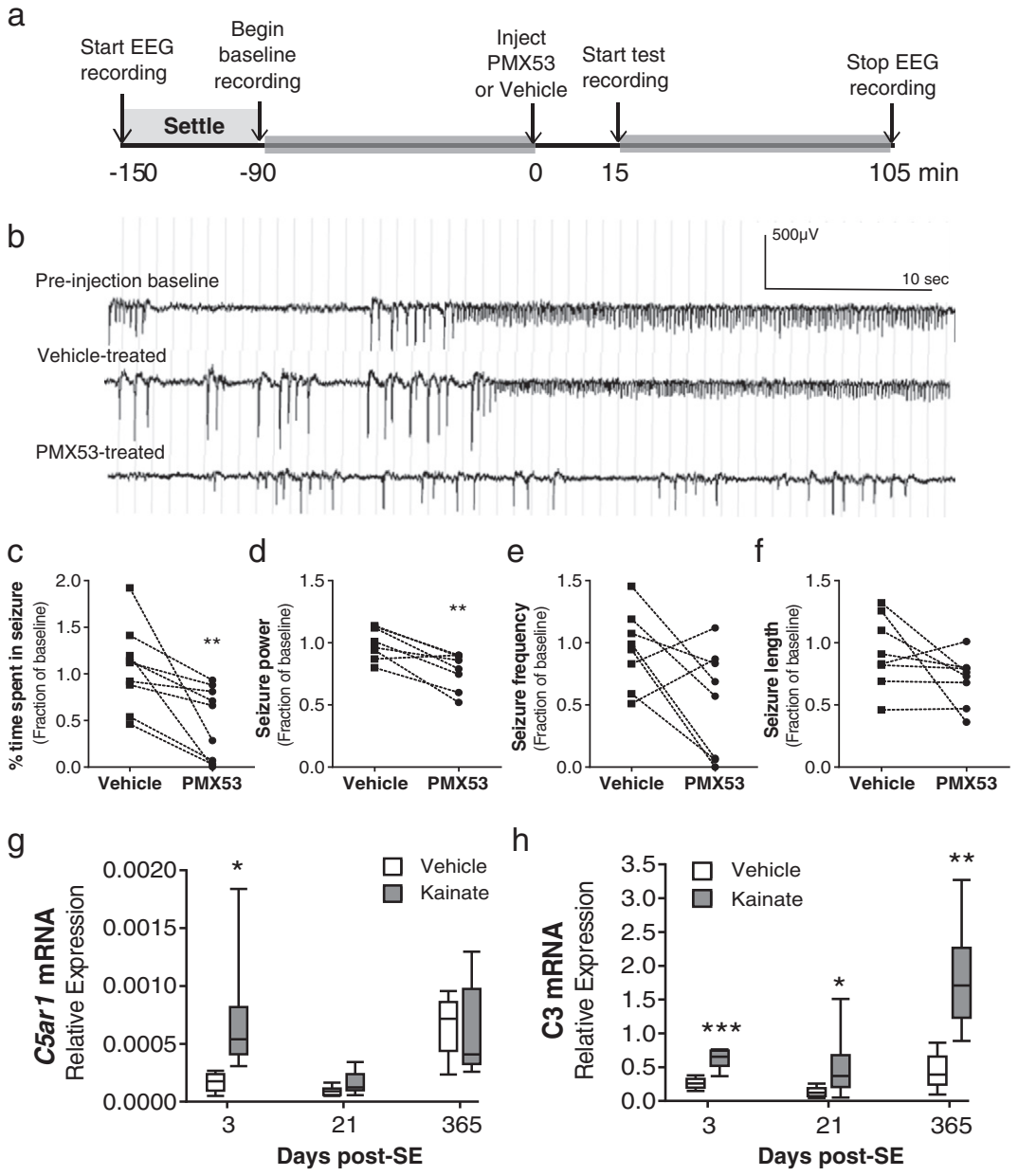

Fig. 2. PMX53 reduces electrographic spontaneous seizures in the chronic *i.h.* kainate model, showing increased complement expression. (a) Experimental injection and recording paradigm. Each mouse received both vehicle and PMX53 with a 1 week washout period in between allowing for paired and blinded comparisons of efficacy. (b) Representative hippocampal EEG traces before and after vehicle and PMX53 treatment. (c) PMX53 treatment resulted in a 58% reduction in overall time spent in seizure with two mice showing complete seizure inhibition ($^{**}P = 0.0087$, $n = 9$). (d) PMX53 treatment caused a 22% reduction in average seizure power or severity compared to vehicle ($^{**}P = 0.0026$, $n = 8$). (e) There was a trend of decreased seizure frequency ($P = 0.053$, $n = 8$), but (f) no change in average seizure length ($P = 0.1221$, $n = 8$). (c–f) Paired student's t-tests were used for analysis. (g, h) Real time PCR of hippocampal RNA from vehicle-injected vs. kainate-SE mice with gene-specific primers revealed upregulation of *C5ar1* mRNA (g); at 3 days ($^{*}P = 0.0253$, $n = 5$–8) but not at 21 days ($P > 0.05$, $n = 6$–14) or 365 days post-SE ($P > 0.05$, $n = 5$–6) and of C3 mRNA at (h) 3 days ($^{***}P < 0.001$, $n = 5$–9), 21 days ($^{*}P = 0.044$, $n = 6$–14) and 365 days post-SE ($^{****}P < 0.0001$, $n = 6$–8). Data presented as Box and Whisker plots showing median and range. Expression of mRNA is relative to housekeeping genes. 2-way ANOVA with Bonferroni multiple comparisons test was used.

of PMX53, where glycine is substituted for D-cyclohexylalanine (PMX203). In contrast to PMX53, no changes in seizure threshold were seen with this inert compound (Fig. 3d). Additionally, the effect of PMX53 was tested in *C5ar1*-deficient mice. PMX53 again elevated the seizure threshold in *C5ar1* wild type mice by 6.1 mA, but no significant protective effects were found in *C5ar1*-deficient and heterozygous mice (Fig. 3e). Interestingly, lack of C5ar1 expression alone did not alter the seizure threshold in a statistically significant manner (Fig. 3e), suggesting that other molecules compensate for the lack of C5ar1 in these animals. Together, these results support that functional C5ar1 is necessary for the anticonvulsant effect of PMX53 in the 6 Hz model.

No effects were seen with PMX53 in either the intravenous pentylenetetrazol (PTZ) or maximal electroshock threshold mouse seizure tests at the same dosage and timepoint (data not shown). Lack of effect in the PTZ model may suggest that acute anticonvulsant action of PMX53 is not through a $GABA_A$ receptor related mechanism.

PMX53 is anti-convulsant in the pilocarpine model of SE leading to subsequently reduced hippocampal neuronal damage

The effect of PMX53 on SE was determined in the pilocarpine model. Injection of PMX53 30 min after pilocarpine administration halved SE-

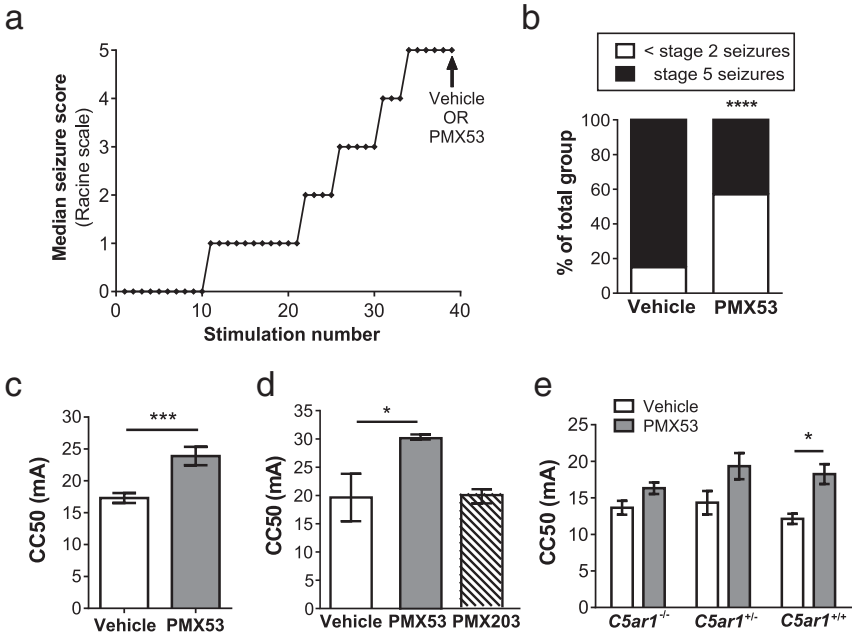

Fig. 3. Anticonvulsant effects of PMX53 in two seizure models; the corneal kindling model and the 6 Hz acute seizure model. (a) Overview of corneal kindling paradigm with median seizure score shown for total group ($n = 30$). (b) 30 min pre-treatment with PMX53 reduced the number of mice with stage 5 seizures by 50% compared to vehicle-injected mice (****$P < 0.0001$, $n = 15$, Fisher's exact test). (c) In the 6 Hz acute seizure model PMX53 pre-treatment significantly increased the critical current at which 50% of the mice seize (CC50) by 6.6 mA (~35%) compared to vehicle (***$P = 0.0003$, $n = 17$, student's t-test). (d) Whilst PMX53 increased the CC50 (*$P = 0.0063$, $n = 15$, one-way ANOVA with $P < 0.05$ Bonferroni post-test), the inert structural analogue PMX203 did not in the 6 Hz model. (e) There was a lack of effect of PMX53 in *C5ar1*-deficient and heterozygote mice in the 6 Hz model, whilst the CC50 was increased by 6.1 mA in *C5ar1*-wild type mice (*$P < 0.05$, $n = 14$, 2-way ANOVA with Bonferroni post-test). Data expressed as mean ± SEM.

associated mortality (Fig. 4a). Furthermore, 30% fewer mice experienced SE, defined as a period of continuous seizure activity lasting >30 min (Fig. 4b), corroborating the anticonvulsant efficacy of PMX53.

When injecting PMX53 15 min prior to pilocarpine (Figs. 4c, d), we could not detect any significant changes in the time to the first seizure or SE induction (Figs. 4e, f). However, there was a >70% decrease in overall SE seizure power evaluated by EEG in PMX53-treated mice (Fig. 4g). Hippocampal neuronal damage was assessed 3 days post-SE using Fluoro-Jade B (FJB) as a marker for degenerating neurons (Fig. 4h). PMX53 treatment prior to SE reduced the number of FJB-positive cells in both the CA1 and CA3 pyramidal areas, by 50% and 75% respectively, but not in the hilus (Fig. 4i). Comparison of *C5ar1*-deficient vs. wild type mice 3 days after pilocarpine-induced SE revealed a significant 40% reduction in FJB-positive cells in the CA3 region in mice lacking the *C5ar1* gene (Fig. 4j). No significant differences were seen in the CA1 region or the hilus between the different genotypes, indicating inflammation-independent cell death mechanisms.

Three days post-SE, we found an 18 fold rise in hippocampal C5ar1 mRNA levels relative to NoSE control mice (Fig. 4k) and a 27 fold increase in C5ar1-immuno-positive microglia, confirming that C5ar1 mRNA is expressed in the post-SE brain at elevated levels indicating a potential role in epileptogenesis (Fig. 4l).

Absence of C5ar1 in the pilocarpine SE model attenuates TNFα increases in microglia

Microglial-specific expression of cytokines TNFα and IL-1β was assessed 3 days post-pilocarpine SE in *C5ar1*-deficient and wild type mice. Initial experiments with *C5ar1*-deficient mice in the pilocarpine model showed no differences from wild type in SE-associated mortality, proportion of mice undergoing SE vs. NoSE or seizure score severity during SE (scored by a modified Racine scale, data not shown).

Proportions of microglia (CD45-intermediate) and infiltrating immune cells (CD45-high) were consistent between genotypes of both SE and NoSE mice (Figs. 5a, b). *C5ar1*-deficient animals showed complete attenuation of TNFα protein increase compared to wild type SE animals (Fig. 5c). No significant differences of IL-1β expression on microglia were observed between genotypes (Fig. 5d). Similarly, changes to IL-6, IL-12 and IL-10 following acute pilocarpine-SE were not different between *C5ar1*-deficient and wild type mice (data not shown).

PMX53 inhibits C5a-induced outward K^+ currents in cultured microglial cells

To activate voltage-gated currents in cultured embryonic-derived forebrain microglial cells, the membrane potential was stepped from a potential of 0 mV to membrane potentials from −70 to +140 mV at 35 mV intervals (Figs. 6a, b, c). In the absence of C5a, hyperpolarising steps activated an inwardly rectifying K^+ current however, after C5a application outward currents at depolarising potentials were significantly increased (Fig. 6d) consistent with the findings of Ilschner et al. (1996). Pre-application of PMX53 (100 nM) prior to C5a applications selectively inhibited the outward C5a-induced currents with no significant differences found between control and PMX53-pre-treated cells (Fig. 6d).

Discussion

In these studies we have shown the therapeutic potential for the inhibition of the innate immune complement receptor C5ar1 as a novel anticonvulsant pathway with possible association to neuroprotective effects.

The ability of PMX53 to significantly increase seizure thresholds and reduce spontaneous recurrent seizures in several murine seizure models suggests that C5ar1 has an important influence on seizures and that C5ar1 inhibition may be a viable strategy to reduce seizure burden in several types of epilepsy. In addition, the increased expression of this receptor at mRNA and protein levels in two chronic epilepsy models is consistent with previous literature (Osaka et al., 1999; Nomaru et al., 2014) and further supports its involvement in epilepsy.

Given the dual efficacy of PMX53 as an anticonvulsant against both acute (6 Hz and pilocarpine models) and chronic seizures (*i.h.* kainate, kindled mice), it is suggested that there may be several mechanisms

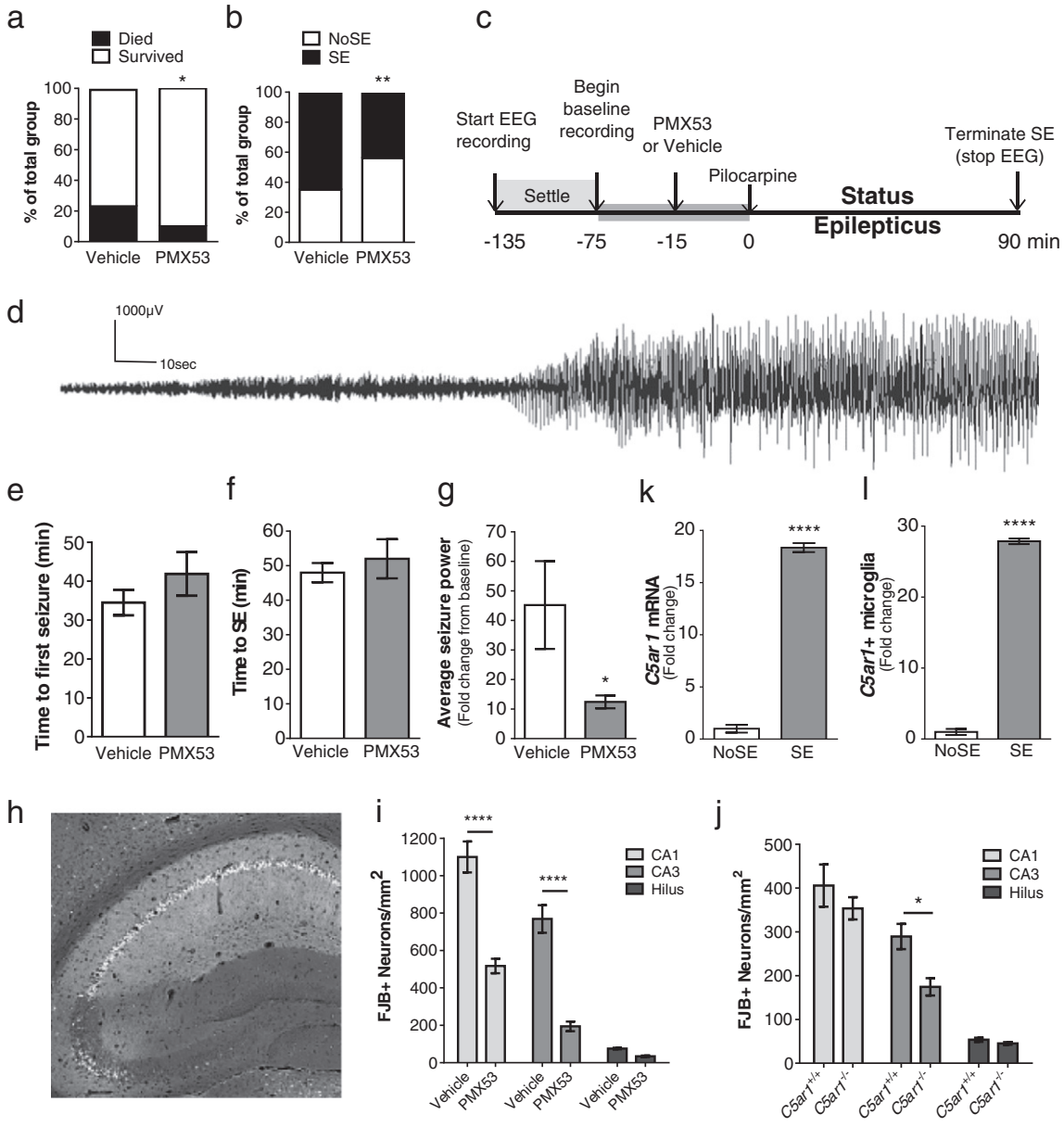

Fig. 4. PMX53 reduced the severity of pilocarpine-induced status epilepticus (SE) and reduced subsequent neuronal loss in the hippocampus 3 days post-SE. (a) PMX53 pre-treatment halved the mortality after pilocarpine injection (*$P = 0.0136$) and (b) reduced the number of mice experiencing SE by 30% (**$P = 0.044$, $n = 20$, both Fisher's exact test). Data expressed as percentage of total group. (c) Drug administration and EEG recording timeline to assess the effect of PMX53 on pilocarpine induced SE. (d) Representative hippocampal EEG recording trace of a mouse reaching SE in the pilocarpine model. PMX53 did not affect the latency to (e) first seizure activity ($P = 0.3243$) or (f) SE ($P = 0.5777$), but reduced (g) EEG power of SE by 73% (*$P = 0.0429$, $n = 5$, student's unpaired two-tailed t-tests for all data). (h) Representative Fluoro-Jade B staining of a hippocampal formation with degenerating neurons at 3 days post-SE. (i) Imaris quantification of FJB-positive neurons per mm^2 revealed a reduction in FJB-positive neurons in CA1 ($P < 0.0001$, $n = 15$–20) and CA3 ($P < 0.0001$, $n = 14$–50), but not the hilus ($P > 0.05$, $n = 13$–15; 2-way ANOVA $P < 0.0001$ with Bonferroni post-tests). (j) After pilocarpine-SE *C5ar1*-deficient mice showed a 40% reduction in FJB-positive neurons in the hippocampal CA3 ($P < 0.05$), but not CA1 area ($P > 0.05$) or the hilus ($P > 0.05$, $n = 14$–18, 2-way ANOVA with Bonferroni post-test; $P = 0.0056$). (k, l) Hippocampal expression of *C5ar1**C5ar1* was increased 3 days after SE relative to NoSE control mice at the mRNA level (k, ****$P < 0.0001$, $n = 9$–11) and in terms of (l) *C5ar1*-immuno-positive microglia (****$P < 0.0001$, $n = 6$, both unpaired, two-tailed student t-tests). Data expressed as mean ± SEM.

of action by which PMX53 can exert its anticonvulsant and potential neuroprotective effects. Primarily, inhibition of inflammation would explain actions against both chronic seizures (*i.h.* kainate and potentially kindled mice) and acute neuronal death (pilocarpine model). However acute anticonvulsant actions in healthy mice are difficult to explain assuming lack of inflammation in the normal brain. It is currently not possible to deduce a definitive mechanism of action from the anticonvulsant profile of a drug, due to the fact that drugs with different mechanisms of action are effective in specific models, indicating that numerous anti-epileptic approaches can block seizures in these animal models. The anticonvulsant profile of PMX53 is similar to that of levetiracetam (Klitgaard et al., 1998), which binds to the synaptic protein SV2a, but in addition is postulated to act via other mechanisms. Lack of effects in the PTZ and MEST models suggest mechanisms of action independent from $GABA_A$ receptors and sodium channels. The *i.h.* kainate model (Wilcox et al., 2013) is resistant to major AEDs, which all inhibit voltage-gated sodium channels. Efficacy of PMX53 in this model therefore advocates that C5ar1 inhibition with PMX53 may be effective against refractory seizures, independent from sodium channel inactivation and $GABA_A$ receptors. Assessment of the impact of PMX53 against chronic seizures in the pilocarpine model, which are known to be more refractory to benzodiazepines, would also be of interest should

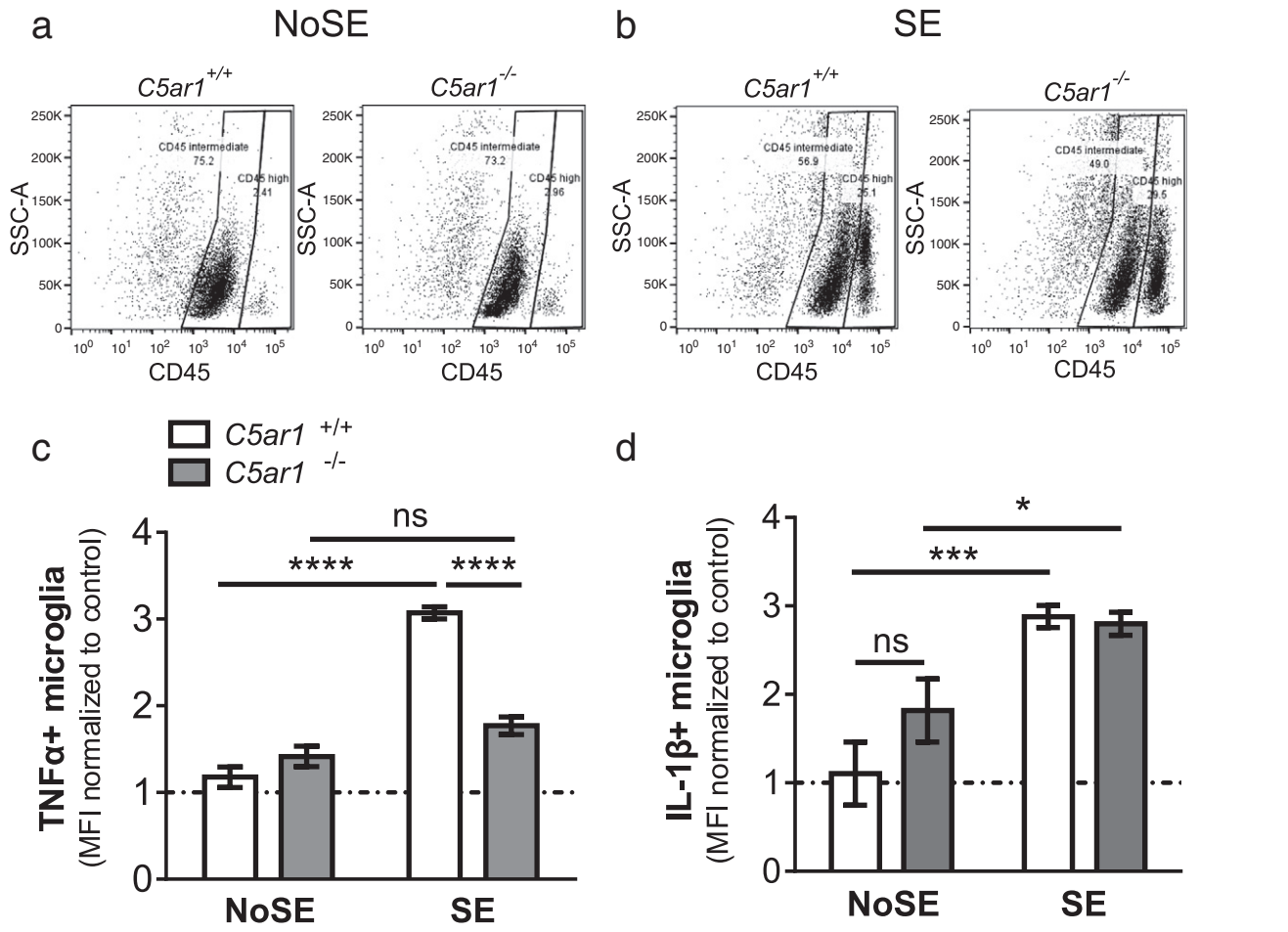

Fig. 5. *C5ar1*-deficiency leads to reduced TNFα expression on microglia 3 days post-pilocarpine SE. (a, b) Representative gating of CD45 positive cells as either CD45-intermediate (microglia) or CD45-high (infiltrating immune cells) by flow cytometry. Both microglial and infiltrating cell populations were consistent in number between genotypes, in both NoSE (a) and SE (b) mice. Values indicate proportion of cell total within each gate. SE mice show a greater proportion of infiltrating cells due to BBB breakdown. (c) Microglial specific expression of TNFα was increased in wild type SE animals compared to NoSE controls (****$P < 0.0001$, $n = 6$) measured by flow cytometry, however *C5ar1*-deficient SE mice showed a non-significant TNFα expression increase compared to NoSE controls ($P > 0.05$, $n = 6$). (d) Microglial expression of IL-1β was increased in SE mice compared to NoSE controls of both wild type (***$P < 0.001$, $n = 6$) and *C5ar1*-deficient mice (*$P < 0.05$, $n = 6$). No significant differences between NoSE or SE groups between each genotype were observed ($P > 0.05$, $n = 6$). 2-way ANOVA with Bonferroni post-tests used for all data sets. Data expressed as mean ± SEM, normalised to naïve control animals of each respective genotype.

further development of this compound occur. Efficacy of PMX53 against seizures such as this would further support C5ar1 inhibition as a novel anticonvulsant pathway.

Based on the premise that seizures cause inflammation that potentiate further seizures (Vezzani et al., 2011), we suggest that C5ar1 antagonism reduces inflammation leading to fewer seizures in the chronic phase. C5ar1 inhibition or absence can reduce the generation of pro-inflammatory cytokines such as TNFα and IL-1β (Lappas et al., 2012), which are known to be pro-convulsant (Vezzani et al., 1999, 2000; Riazi et al., 2008), and we propose a similar mechanism in this study. This effect on inflammation is consistent with our finding that C5ar1 is expressed on microglial cells and that 1) PMX53 reduces C5a-induced outward potassium currents and 2) *C5ar1* absence leads to attenuation of SE-induced microglial TNFα upregulation, indicating that C5ar1-mediated release of microglial TNFα and/or potassium may be a contributor to seizures and subsequent neuronal damage. Furthermore, it has been shown in several cell types, including macrophages and dendritic cells, that C5a/C5ar1 activation drives production of pro-inflammatory cytokines, such as TNFα and IL-1β, through NFκB activation (O'Barr and Cooper, 2000; Kastl et al., 2006; Lappas et al., 2012).

TNFα is a key pro-inflammatory and pro-convulsant mediator (Balosso et al., 2013). Microglial specific expression of TNFα induced by peripheral inflammation caused a significant decrease in seizure thresholds of rats in the *i.v.* PTZ seizure test (Riazi et al., 2008). The mechanisms by which TNFα can affect brain excitability have been well studied and include promotion of increased synaptic AMPA receptor availability (Beattle et al., 2002), endocytosis of $GABA_A$ receptors (Stellwagen et al., 2005) and alterations to glutamate uptake and release by glia through CXCR4 signalling (Bezzi et al., 2001).

Furthermore, there is extensive evidence that inhibition of IL-1β is anticonvulsant and neuroprotective in rodent models and that C5ar1 can drive IL-1β expression through the NFκB pathway (Lappas et al., 2012). Direct effects of IL-1β on neuronal excitation, via activation of *Src* kinase, causing NMDA receptor activation were shown leading to calcium flux into neuronal cells promoting excitotoxicity and seizures (Viviani et al., 2003; Balosso et al., 2008). Similar to TNFα, IL-1β is also thought to affect excitability through inhibition of glutamate uptake by astrocytes (Hu et al., 2000). Even though no changes to IL-1β levels were observed in *C5ar1*-deficient compared to wild type post-SE mice, it is possible that this cytokine is still playing a role in earlier and/or later stage inflammatory events promoting excitation, which may be mediated in part by C5ar1.

Reduction of C5ar1-mediated NFκB signalling may also contribute to potential neuroprotection, as seen in the pilocarpine-SE model. In addition to the decreased SE seizure power found with PMX53, reduction of NFκB signalling would improve neuronal survival as inflammation is thought to contribute significantly to neuronal death. This is due to production of pro-inflammatory cytokines, such as IL-1β and TNFα, which

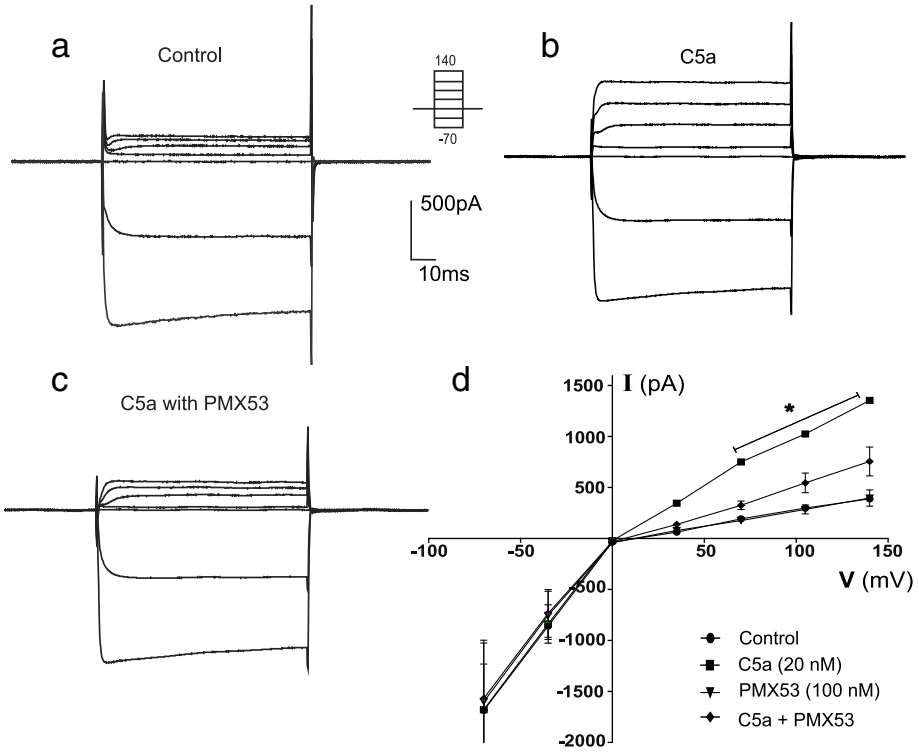

Fig. 6. C5a application induced outward rectifying K^+ currents in mouse microglial cells which was inhibited by PMX53. (a) Inwardly rectifying K^+ currents recorded from a microglial cell without stimulation by C5a. During this time, the holding potential was 0 mV and voltage steps of 100 ms duration to potentials from −70 to +140 mV with a 35 mV increment were applied. The stimulation protocol is presented in the inset. (b) Recording from the same cell after 20 nM C5a application. (c) Current trace from the same cell pre-applied with PMX (100 nM) followed by C5a application (20 nM). (d) Averaged current–voltage curves. C5a (squares) at 20 nM exhibited a significant increase ($^*P < 0.05$, $n = 4$) in outward rectifying currents as compared to control (circles). Pre-application of PMX53 (100 nM, diamonds) inhibited the C5a-induced outward current in microglia ($P > 0.05$ as compared to C5a-only and control stimulations). PMX53 application had no effect on baseline current (triangle). One way ANOVA with Bonferroni post-hoc multiple comparisons test used for analysis. Data shown as mean ± SEM ($n = 4$–5 cells per group).

have been shown previously to be toxic to neurons (Thornton et al., 2006). It must be made clear however, that reduced neuronal death in PMX53-treated mice following pilocarpine-SE can be attributed to the anticonvulsant actions of PMX53, however this same statement does not hold true for *C5ar1*-deficient mice which showed no difference in SE or seizure severity compared to wild type mice following pilocarpine. Lack of altered SE in *C5ar1*-deficient mice is consistent with results from the 6 Hz study showing that vehicle-treated *C5ar1*-deficient and wild type mice had consistent seizure thresholds (CC50) therefore *C5ar1*-deficiency alone did not alter seizure response. For this reason reduced neuronal damage in *C5ar1*-deficient mice following pilocarpine may be attributed to a neuroprotective role of inhibiting C5ar1 and not due to anticonvulsant actions. The putative neuroprotective mechanism of C5ar1 inhibition during SE suggested here is similar to that found in several disease models (Woodruff et al., 2010), and may also be related to improved preservation of the blood brain barrier during prolonged seizures.

In rodents, SE is known to harm the integrity of the blood brain barrier. Also, the extent of blood brain barrier damage, induced by seizures or mannitol treatment, correlated positively with increased spontaneous and induced seizures (Van Vliet et al., 2007; Fabene et al., 2008). PMX53 was previously shown to block NFκB translocation to the nucleus in mouse brain microvascular endothelial cells treated with mouse serum containing high levels of endogenous C5a (Jacob et al., 2011). This prevented transcription of inflammatory mediators, maintained expression of ZO-1, a key tight junction scaffolding protein of the blood brain barrier, and reduced caspase-3 activity of endothelial cells thereby decreasing apoptosis and improving blood brain barrier integrity (Jacob et al., 2011). These findings collectively signal that C5ar1 inhibition may contribute to preserving blood brain barrier integrity during SE, thus reducing SE severity as well as neuronal damage and potentially lessening spontaneous seizure development and/or improving disease outcomes. The latter outcomes still need to be investigated.

Additionally, the effect of C5ar1 activation on neurons is of interest in regards to the reduced neuronal loss in CA1 and CA3 seen with C5ar1 inhibition or absence prior to pilocarpine SE. C5a treatment of cultured murine neurons was shown to induce apoptosis, which was reduced with PMX53 pre-treatment and *C5ar1*-deficiency (Pavlovski et al., 2012). Despite the difficulty to assess the extent to which contaminating microglia and astrocytes contributed to these effects, these data confirm that C5ar1 inhibition is beneficial to neuronal survival and hence may suggest a neuroprotective contribution of inhibiting C5ar1 signalling in the pilocarpine model, which is in addition to reduced seizures via anticonvulsant mechanisms. In order to fully define and confirm neuroprotective potential of C5ar1 inhibition, treatment with PMX53 following termination of pilocarpine-SE would be required. Such experiments are planned in the future.

The anticonvulsant mechanism of PMX53 in the acute 6 Hz seizure model may seem difficult to explain due to the expected lack of inflammation in the animals. However, neuro-modulatory actions of IL-1β and TNFα in normal brain have been previously reviewed (Vitkovic et al., 2000). Similar to our data with C5ar1 inhibition, blockade of IL-1β actions either through direct receptor antagonism (anti-IL-1ra) or inhibition of caspase-1 (the interleukin-converting enzyme) was anticonvulsant in both the acute bicuculline and kainic acid rodent models of acute seizures (Vezzani et al., 1999, 2000), as well as in chronic epilepsy models (Vezzani et al., 2000; Maroso et al., 2011). This reveals that acute cytokine inhibition in normal brain can reduce excitability and increase seizure thresholds (Vitkovic et al., 2000).

An additional potential anticonvulsant mechanism to explain actions of PMX53 in acute seizure tests is related specifically to C5ar1 expressed by microglia. In microglia, C5a can stimulate outward

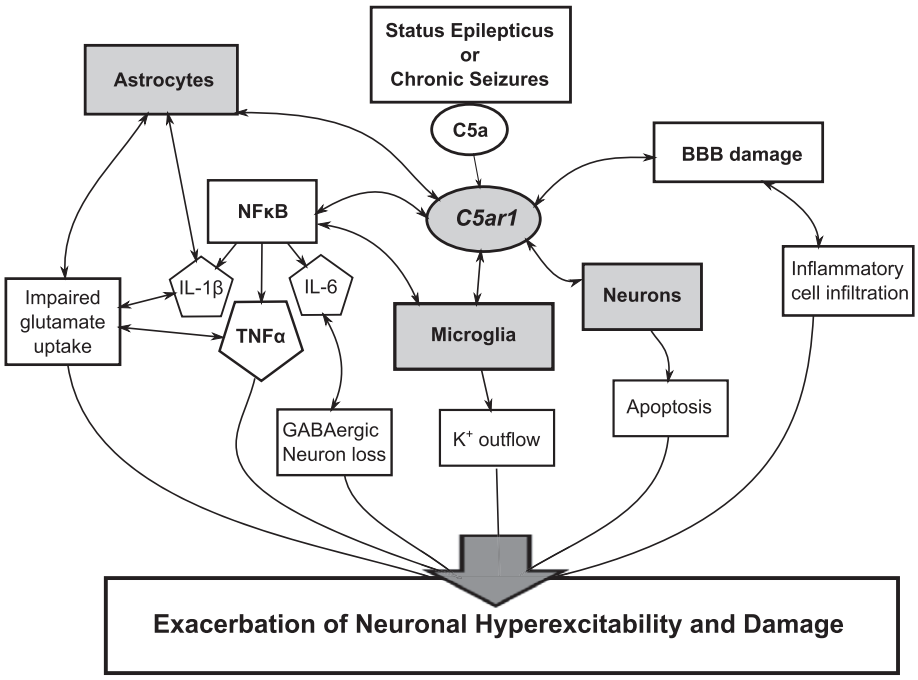

Fig. 7. A proposed mechanism of C5ar1 involvement in seizure initiation and neuronal hyper-excitability and damage. Increases in C5a driven by seizures or status epilepticus (SE) lead to C5ar1 activation which modulates multiple pathways affecting neuronal hyper-excitability and damage. These pathways include NFκB-mediated production of pro-inflammatory cytokines including TNFα, IL-1β and IL-6, which have each been shown to have proconvulsant actions in a variety of seizure models. C5ar1 activation is also known to affect all brain cell types and causes apoptosis in neurons, changes K^+ channel outflow in microglia and potentially indirectly impairs glutamate uptake and release in astrocytes through TNFα. Additionally, deleterious effects of C5ar1 activation in endothelial cells alter BBB integrity potentially leading to increased inflammatory cell infiltration, perpetuating further CNS inflammation. We propose that inhibition of C5ar1 reduces the extent of inflammation and lessens neuronal hyper-excitability and subsequent excitotoxic damage through some of these mechanistic pathways.

rectifying K^+ currents through C5ar1 binding (Ilschner et al., 1996), which may contribute to neuronal excitation if microglia are in close proximity to neuronal membranes, that are highly sensitive to depolarisation. PMX53 was shown to inhibit this outward current therefore preventing destabilisation of extracellular K^+ homeostasis and potentially providing a possible explanation as to how PMX53 can increase acute seizure thresholds.

Clinically PMX53 has previously been trialled as a dermal cream for inflammatory psoriasis and as an oral treatment for chronic rheumatoid arthritis (Ji et al., 2002; Koehl, 2006). In both trials, PMX53 passed safety and tolerability barriers, with apparent efficacy in the psoriasis, but not rheumatoid arthritis study (Koehl, 2006; Vergunst et al., 2007). These data support that chronic C5ar1 antagonism is not deleterious in itself, which is key for future drug development. Furthermore, a C5a antibody, Eculizumab, is currently used in the clinic for a rare immunological condition, paroxysmal nocturnal hemoglobinuria (Hillmen et al., 2006), further supporting that C5ar1 pathway inhibition is safe. However, due to the short half-life of PMX53, newer brain-permeable C5ar1 inhibitors with an improved pharmacokinetic profile would need to be developed.

Conclusions

In conclusion, this work has demonstrated a pathogenic role of complement C5ar1 signalling in seizure initiation and severity as well as SE-induced neuronal degeneration. From these studies the definitive mechanisms of anticonvulsant action for PMX53 are still unclear. However, this work has outlined that inflammatory cytokine expression and modulation of microglial potassium channels are affected by C5ar1 absence or inhibition by PMX53 and may be part of a larger mechanism of action (Fig. 7). Given the efficacy of PMX53 in refractory seizure models, our findings provide a novel target for future AED development, which may be effective for pharmaco-resistant seizure types.

Acknowledgments

This work was supported by grants 63145 and 1044407 (KB) from the Australian National Health and Medical Research Council and also funding from Australian Rotary Health and the Rotary Club of Koo Wee Rup—Lang Lang. We thank David She for kindling of the mice, Kah Ni Tan for assistance with qPCR, Dr. Detlev Boison and Dr. Panos Theofilas for teaching of the *i.h.* kainate model and EEG and finally Dr. Silvia Manzanero for her assistance with flow cytometry experiments. All authors declare they have no conflicts of interest related to this study.

References

Amara, U., Flierl, M.A., Rittirsch, D., Klos, A., Chen, H., Acker, B., Brückner, U.B., Nilsson, B., Gebhard, F., Lambris, J.D., 2010. Molecular intercommunication between the complement and coagulation systems. J. Immunol. 185, 5628–5636.

Aronica, E., Boer, K., van Vliet, E.A., Redeker, S., Baayen, J.C., Spliet, W.G., van Rijen, P.C., Troost, D., da Silva, F.H., Wadman, W.J., Gorter, J.A., 2007. Complement activation in experimental and human temporal lobe epilepsy. Neurobiol. Dis. 26, 497–511.

Balosso, S., Maroso, M., Sanchez-Alavez, M., Ravizza, T., Frasca, A., Bartfai, T., Vezzani, A., 2008. A novel non-transcriptional pathway mediates the proconvulsive effects of interleukin-1beta. Brain 131, 3256–3265.

Balosso, S., Ravizza, T., Aronica, E., Vezzani, A., 2013. The dual role of TNF-α and its receptors in seizures. Exp. Neurol. 247, 267–271.

Başaran, N., Hincal, F., Kansu, E., Cidot er, A., 1994. Humoral and cellular immune parameters in untreated and phenytoin- or carbamazepine-treated epileptic patients. Int. J. Immunopharmacol. 16, 1071–1077.

Beattle, E.C., Stellwagen, D., Morishita, W., Bresnahan, J.C., Ha, B.K., Mark von, Z., Beattie, M.S., Malenka, R.C., 2002. Control of synaptic strength by glial TNFα. Science 295, 2282–2285.

Becker, A.J., Chen, J., Zien, A., Sochivko, D., Normann, S., Schramm, J., Elger, C.E., Wiestler, O.D., Blumcke, I., 2003. Correlated stage- and subfield-associated hippocampal gene expression patterns in experimental and human temporal lobe epilepsy. Eur. J. Neurosci. 18, 2792–2802.

Bezzi, P., Domercq, M., Brambilla, L., Galli, R., Schols, D., De Clercq, E., Vescovi, A., Bagetta, G., Kollias, G., Meldolesi, J., 2001. CXCR4-activated astrocyte glutamate release via TNFα: amplification by microglia triggers neurotoxicity. Nat. Neurosci. 4, 702–710.

Borges, K., Gearing, M., McDermott, D.L., Smith, A.B., Almonte, A.G., Wainer, B.H., Dingledine, R., 2003. Neuronal and glial pathological changes during epileptogenesis in the mouse pilocarpine model. Exp. Neurol. 182, 21–34.

Fabene, P.F., Navarro Mora, G., Martinello, M., Rossi, B., Merigo, F., Ottoboni, L., Bach, S., Angiari, S., Benati, D., Chakir, A., Zanetti, L., Schio, F., Osculati, A., Marzola, P., Nicolato, E., Homeister, J.W., Xia, L., Lowe, J.B., McEver, R.P., Osculati, F., Sbarbati, A., Butcher, E.C., Constantin, G., 2008. A role for leukocyte-endothelial adhesion mechanisms in epilepsy. Nat. Med. 14, 1377–1383.

Finch, A.M., Wong, A.K., Paczkowski, N.J., Wadi, S.K., Craik, D.J., Fairlie, D.P., Taylor, S.M., 1999. Low-molecular-weight peptidic and cyclic antagonists of the receptor for the complement factor C5a. J. Med. Chem. 42, 1965–1974.

Gorter, J.A., van Vliet, E.A., Aronica, E., Breit, T., Rauwerda, H., da Silva, F.H.L., Wadman, W.J., 2006. Potential new antiepileptogenic targets indicated by microarray analysis in a rat model for temporal lobe epilepsy. J. Neurosci. 26, 11083–11110.

Gouder, N., Fritschy, J.M., Boison, D., 2003. Seizure suppression by adenosine A1 receptor activation in a mouse model of pharmacoresistant epilepsy. Epilepsia 44, 877–885.

Hillmen, P., Young, N.S., Schubert, J., Brodsky, R.A., Socié, G., Muus, P., Röth, A., Szer, J., Elebute, M.O., Nakamura, R., 2006. The complement inhibitor eculizumab in paroxysmal nocturnal hemoglobinuria. N. Engl. J. Med. 355, 1233–1243.

Hodson, M.P., Dear, G.J., Griffin, J.L., Haselden, J.N., 2009. An approach for the development and selection of chromatographic methods for high-throughput metabolomic screening of urine by ultra pressure LC–ESI-ToF-MS. Metabolomics 5, 166–182.

Hollmann, T.J., Mueller-Ortiz, S.L., Braun, M.C., Wetsel, R.A., 2008. Disruption of the C5a receptor gene increases resistance to acute gram-negative bacteremia and endotoxic shock: opposing roles of C3a and C5a. Mol. Immunol. 45, 1907–1915.

Hu, S., Sheng, W.S., Ehrlich, L.C., Peterson, P.K., Chao, C.C., 2000. Cytokine effects on glutamate uptake by human astrocytes. Neuroimmunomodulation 7, 153–159.

Ilschner, S., Nolte, C., Kettenmann, H., 1996. Complement factor C5a and epidermal growth factor trigger the activation of outward potassium currents in cultured murine microglia. Neuroscience 73, 1109–1120.

Jacob, A., Hack, B., Chen, P., Quigg, R.J., Alexander, J.J., 2011. C5a/CD88 signaling alters blood–brain barrier integrity in lupus through nuclear factor-kappaB. J. Neurochem. 119, 1041–1051.

Jamali, S., Bartolomei, F., Robaglia-Schlupp, A., Massacrier, A., Peragut, J.C., Regis, J., Dufour, H., Ravid, R., Roll, P., Pereira, S., Royer, B., Roeckel-Trevisiol, N., Fontaine, M., Guye, M., Boucraut, J., Chauvel, P., Cau, P., Szepetowski, P., 2006. Large-scale expression study of human mesial temporal lobe epilepsy: evidence for dysregulation of the neurotransmission and complement systems in the entorhinal cortex. Brain 129, 625–641.

Jamali, S., Salzmann, A., Perroud, N., Ponsole-Lenfant, M., Cillario, J., Roll, P., Roeckel-Trevisiol, N., Crespel, A., Balzar, J., Schlachter, K., 2010. Functional variant in complement C3 gene promoter and genetic susceptibility to temporal lobe epilepsy and febrile seizures. PLoS ONE 5, e12740.

Ji, H., Ohmura, K., Mahmood, U., Lee, D.M., Hofhuis, F., Boackle, S.A., Takahashi, K., Holers, V.M., Walport, M., Gerard, C., 2002. Arthritis critically dependent on innate immune system players. Immunity 16, 157–168.

Kastl, S., Speidl, W., Kaun, C., Rega, G., Assadian, A., Weiss, T., Valent, P., Hagmueller, G., Maurer, G., Huber, K., 2006. The complement component C5a induces the expression of plasminogen activator inhibitor-1 in human macrophages via NF-κB activation. J. Thromb. Haemost. 4, 1790–1797.

Kharatishvili, I., Shan, Z.Y., She, D.T., Foong, S., Kurniawan, N.D., Reutens, D.C., 2014. MRI changes and complement activation correlate with epileptogenicity in a mouse model of temporal lobe epilepsy. Brain Struct. Funct. 219, 683–706.

Kim, G.H., Mocco, J., Hahn, D.K., Kellner, C.P., Komotar, R.J., Ducruet, A.F., Mack, W.J., Connolly Jr., E.S., 2008. Protective effect of C5a receptor inhibition after murine reperfused stroke. Neurosurgery 63, 122.

Klitgaard, H., Matagne, A., Gobert, J., Wülfert, E., 1998. Evidence for a unique profile of levetiracetam in rodent models of seizures and epilepsy. Eur. J. Pharmacol. 353, 191–206.

Koehl, J., 2006. Drug evaluation: the C5a receptor antagonist PMX-53. Curr. Opin. Mol. Ther. 8, 529–538.

Kwan, P., Schachter, S.C., Brodie, M.J., 2011. Drug-resistant epilepsy. N. Engl. J. Med. 365, 919–926.

Lappas, M., Woodruff, T.M., Taylor, S.M., Permezel, M., 2012. Complement C5a regulates prolabor mediators in human placenta. Biol. Reprod. 86, 190.

Li, L., Z-y, Xiong, Qian, Z.M., T-z, Zhao, Feng, H., Hu, S., Hu, R., Ke, Y., Lin, J., 2014. Complement C5a is detrimental to histological and functional locomotor recovery after spinal cord injury in mice. Neurobiol. Dis. 66, 74–82.

March, D.R., Proctor, L.M., Stoermer, M.J., Sbaglia, R., Abbenante, G., Reid, R.C., Woodruff, T.M., Wadi, K., Paczkowski, N., Tyndall, J.D., 2004. Potent cyclic antagonists of the complement C5a receptor on human polymorphonuclear leukocytes. Relationships between structures and activity. Mol. Pharmacol. 65, 868–879.

Marchi, N., Granata, T., Freri, E., Ciusani, E., Ragona, F., Puvenna, V., Teng, Q., Alexopolous, A., Janigro, D., 2011. Efficacy of anti-inflammatory therapy in a model of acute seizures and in a population of pediatric drug resistant epileptics. PLoS ONE 6, e18200.

Maroso, M., Balosso, S., Ravizza, T., Iori, V., Wright, C.I., French, J., Vezzani, A., 2011. Interleukin-1β biosynthesis inhibition reduces acute seizures and drug resistant chronic epileptic activity in mice. Neurotherapeutics 8, 304–315.

Nomaru, H., Sakumi, K., Katogi, A., Ohnishi, Y.N., Kajitani, K., Tsuchimoto, D., Nestler, E.J., Nakabeppu, Y., 2014. Fosb gene products contribute to excitotoxic microglial activation by regulating the expression of complement C5a receptors in microglia. Glia 62 (8), 1284–1298.

O'Barr, S., Cooper, N.R., 2000. The C5a complement activation peptide increases IL-1β and IL-6 release from amyloid-β primed human monocytes: implications for Alzheimer's disease. J. Neuroimmunol. 109, 87–94.

Osaka, H., McGinty, A., Hoepken, U., Lu, B., Gerard, C., Pasinetti, G., 1999. Expression of C5a receptor in mouse brain: role in signal transduction and neurodegeneration. Neuroscience 88, 1073–1082.

Pavlovski, D., Thundyil, J., Monk, P.N., Wetsel, R.A., Taylor, S.M., Woodruff, T.M., 2012. Generation of complement component C5a by ischemic neurons promotes neuronal apoptosis. FASEB J. 26, 3680–3690.

Riazi, K., Galic, M.A., Kuzmiski, J.B., Ho, W., Sharkey, K.A., Pittman, Q.J., 2008. Microglial activation and TNFα production mediate altered CNS excitability following peripheral inflammation. Proc. Natl. Acad. Sci. 105, 17151–17156.

Samala, R., Willis, S., Borges, K., 2008. Anticonvulsant profile of a balanced ketogenic diet in acute mouse seizure models. Epilepsy Res. 81, 119–127.

Sangster, T., Major, H., Plumb, R., Wilson, A.J., Wilson, I.D., 2006. A pragmatic and readily implemented quality control strategy for HPLC–MS and GC–MS-based metabonomic analysis. Analyst 131, 1075–1078.

Schmued, L.C., Hopkins, K.J., 2000. Fluoro-Jade B: a high affinity fluorescent marker for the localization of neuronal degeneration. Brain Res. 874, 123–130.

Scola, A.-M., Higginbottom, A., Partridge, L.J., Reid, R.C., Woodruff, T., Taylor, S.M., Fairlie, D.P., Monk, P.N., 2007. The role of the N-terminal domain of the complement fragment receptor C5L2 in ligand binding. J. Biol. Chem. 282, 3664–3671.

Sewell, D.L., Nacewicz, B., Liu, F., Macvilay, S., Erdei, A., Lambris, J.D., Sandor, M., Fabry, Z., 2004. Complement C3 and C5 play critical roles in traumatic brain cryoinjury: blocking effects on neutrophil extravasation by C5a receptor antagonist. J. Neuroimmunol. 155, 55–63.

Smeland, O.B., Hadera, M.G., McDonald, T.S., Sonnewald, U., Borges, K., 2013. Brain mitochondrial metabolic dysfunction and glutamate level reduction in the pilocarpine model of temporal lobe epilepsy in mice. J. Cereb. Blood Flow Metab. 33, 1090–1097.

Stellwagen, D., Beattie, E.C., Seo, J.Y., Malenka, R.C., 2005. Differential regulation of AMPA receptor and GABA receptor trafficking by tumor necrosis factor-α. J. Neurosci. 25, 3219–3228.

Strachan, A.J., Shiels, I.A., Reid, R.C., Fairlie, D.P., Taylor, S.M., 2001. Inhibition of immune-complex mediated dermal inflammation in rats following either oral or topical administration of a small molecule C5a receptor antagonist. Br. J. Pharmacol. 134, 1778–1786.

Thomas, N.K., Willis, S., Sweetman, L., Borges, K., 2012. Triheptanoin in acute mouse seizure models. Epilepsy Res. 99, 312–317.

Thornton, P., Pinteaux, E., Gibson, R.M., Allan, S.M., Rothwell, N.J., 2006. Interleukin-1-induced neurotoxicity is mediated by glia and requires caspase activation and free radical release. J. Neurochem. 98, 258–266.

Van Vliet, E., da Costa, Araujo S., Redeker, S., Van Schaik, R., Aronica, E., Gorter, J., 2007. Blood–brain barrier leakage may lead to progression of temporal lobe epilepsy. Brain 130, 521–534.

Vergunst, C.E., Gerlag, D.M., Dinant, H., Schulz, L., Vinkenoog, M., Smeets, T.J., Sanders, M.E., Reedquist, K.A., Tak, P.P., 2007. Blocking the receptor for C5a in patients with rheumatoid arthritis does not reduce synovial inflammation. Rheumatology 46, 1773–1778.

Vezzani, A., Granata, T., 2005. Brain inflammation in epilepsy: experimental and clinical evidence. Epilepsia 46, 1724–1743.

Vezzani, A., Conti, M., De Luigi, A., Ravizza, T., Moneta, D., Marchesi, F., De Simoni, M.G., 1999. Interleukin-1β immunoreactivity and microglia are enhanced in the rat hippocampus by focal kainate application: functional evidence for enhancement of electrographic seizures. J. Neurosci. 19, 5054–5065.

Vezzani, A., Moneta, D., Conti, M., Richichi, C., Ravizza, T., De Luigi, A., De Simoni, M., Sperk, G., Andell-Jonsson, S., Lundkvist, J., 2000. Powerful anticonvulsant action of IL-1 receptor antagonist on intracerebral injection and astrocytic overexpression in mice. Proc. Natl. Acad. Sci. 97, 11534–11539.

Vezzani, A., French, J., Bartfai, T., Baram, T.Z., 2011. The role of inflammation in epilepsy. Nat. Rev. Neurol. 7, 31–40.

Vitkovic, L., Bockaert, J., Jacque, C., 2000. "Inflammatory" cytokines. J. Neurochem. 74, 457–471.

Viviani, B., Bartesaghi, S., Gardoni, F., Vezzani, A., Behrens, M., Bartfai, T., Binaglia, M., Corsini, E., Di Luca, M., Galli, C., 2003. Interleukin-1β enhances NMDA receptor-mediated intracellular calcium increase through activation of the Src family of kinases. J. Neurosci. 23, 8692–8700.

Wilcox, K.S., Dixon-Salazar, T., Sills, G.J., Ben-Menachem, E., Steve White, H., Porter, R.J., Dichter, M.A., Moshé, S.L., Noebels, J.L., Privitera, M.D., Rogawski, M.A., 2013. Issues related to development of new antiseizure treatments. Epilepsia 54, 24–34.

Willis, S., Stoll, J., Sweetman, L., Borges, K., 2010. Anticonvulsant effects of a triheptanoin diet in two mouse chronic seizure models. Neurobiol. Dis. 40, 565–572.

Wong, A.K., Finch, A.M., Pierens, G.K., Craik, D.J., Taylor, S.M., Fairlie, D.P., 1998. Small molecular probes for G-protein-coupled C5a receptors: conformationally constrained antagonists derived from the C terminus of the human plasma protein C5a. J. Med. Chem. 41, 3417–3425.

Woodruff, T.M., Pollitt, S., Proctor, L.M., Stocks, S.Z., Manthey, H.D., Williams, H.M., Mahadevan, I.B., Shiels, I.A., Taylor, S.M., 2005. Increased potency of a novel complement factor 5a receptor antagonist in a rat model of inflammatory bowel disease. J. Pharmacol. Exp. Ther. 314, 811–817.

Woodruff, T.M., Crane, J.W., Proctor, L.M., Buller, K.M., Shek, A.B., De Vos, K., Pollitt, S., Williams, H.M., Shiels, I.A., Monk, P.N., 2006. Therapeutic activity of C5a receptor antagonists in a rat model of neurodegeneration. FASEB J. 20, 1407–1417.

Woodruff, T.M., Costantini, K.J., Crane, J.W., Atkin, J.D., Monk, P.N., Taylor, S.M., Noakes, P.G., 2008. The complement factor C5a contributes to pathology in a rat model of amyotrophic lateral sclerosis. J. Immunol. 181, 8727–8734.

Woodruff, T.M., Ager, R.R., Tenner, A.J., Noakes, P.G., Taylor, S.M., 2010. The role of the complement system and the activation fragment C5a in the central nervous system. Neruomol. Med. 12, 179–192.

Xiong, Z.Q., Qian, W., Suzuki, K., McNamara, J.O., 2003. Formation of complement membrane attack complex in mammalian cerebral cortex evokes seizures and neurodegeneration. J. Neurosci. 23, 955–960.